Supporting Information

Mohajerani et al. 10.1073/pnas.1101914108

SI Methods

Animal Model. Adult male C57BL6J mice were used ($n = 32$) for most experiments, whereas I/LnJ acallosal mice ($n = 7$; Jackson Laboratory) were used for a subset of these experiments. Animal protocols were approved by the University of British Columbia Animal Care Committee. Anesthesia was induced with urethane (0.12% wt/wt), and body temperature was maintained at 37 ± 0.5 °C with the use of a feedback-controlled heating pad. A large (7 × 8 mm; bregma 2.5 to −4.5 mm and lateral 0–4 mm) bilateral cranial window was surgically created, and the dura matter was carefully removed to expose a large region of cortex as described (1).

Voltage-Sensitive Dye Imaging. For in vivo voltage-sensitive dye (VSD) imaging, the dye, RH1692 (Optical Imaging) (2), was dissolved in the Hepes-buffered saline: optical density of 5–7 (measured at 550 nm) was applied to the exposed cortex for 60–90 min. To minimize movement artifacts caused by respiration, the brain was covered with 1.5% agarose made in Hepes-buffered saline and sealed with a glass coverslip. Respiratory rhythm was measured using a motion sensor and indicated no contribution of breathing-induced hemodynamic signals or motion artifacts to VSD signals (1). For VSD data collection, 12-bit images were captured with either 5- or 6.67-ms resolution with a CCD camera (1M60 Pantera; Dalsa) and an EPIX E1DB frame grabber with XCAP 3.1 imaging software (EPIX, Inc.). VSD was excited with a red LED (627-nm center; Luxeon K2) and fluorescence filters as described (1). Images were taken through a macroscope composed of front to front video lenses (8.6 × 8.6-mm field of view, 67 μm/pixel). To measure cortical activity evoked by sensory stimulation, we stimulated the hind- and forelimbs using a piezoelectric device (Q220-AY-203YB; Piezo Systems) using single 5-ms taps.

Mini-Stroke Procedure. Focal photothrombotic stroke was targeted to a single surface arteriole within the right hemisphere forelimb somatosensory cortex as described (3–5). The arteriole was selected based on its appearance and position within the anterior segment of the forelimb somatosensory VSD map. To induce occlusion, we injected the photosenstizer Rose Bengal (Na^+ salt, R3877; Sigma) diluted to 10 mg/mL in Hepes buffered saline into the tail vein at 30 μg/g mouse body weight. Within 10 min of injection, an individual surface arteriole (averaging 28.9 ± 1.6 μm in diameter, $n = 25$) (Fig. S1) was targeted for occlusion using 0.7–1.4 mW of 532-nm laser light (MGM-20; Beta Electronics). The laser was coupled through the microscope's epifluorescence light path and focused to a spot through a 40× 0.8-NA water immersion lens as described (3). The targeted arteriole was illuminated until a stable clot formed.

Speckle Imaging. To confirm occlusion of targeted arterioles, we examined cortical blood flow with laser speckle contrast imaging (6) as previously described (3). For illumination, a 784-nm 32-mW StockerYale SNF-XXX-785S-35 laser (Stocker & Yale) with an Edmund anamorphic beam expander T47274 (Edmund Optics) was held directly on a micromanipulator at an angle of 30°, directed at the brain surface that was enclosed by a coverslip and agarose, and viewed with a 4× 0.075-NA objective. We recorded images with a Dalsa 1M60 Pantera camera (Dalsa) mounted on the upright microscope used for photoactivation. We collected 50 image time sequences at 10 Hz by using 10-ms exposures. Individual images of variance were created in ImageJ (National Institutes of Health) using its 2D variance filter (3 × 3- or 5 × 5-pixel kernel size, 3.47 μm/pixel). After variance filtering, all images were averaged, and a single 32-bit image of the SD was produced by taking the square root of the averaged variance image. The SD image was then divided by the mean of all of the raw images to help correct for uneven illumination and create an image of speckle contrast (SD/mean).

Data Analysis. VSD responses to sensory-evoked stimulation were calculated as the normalized difference to the average baseline recorded before stimulation ($\Delta F/F_0 \times 100$) using custom-written code in Matlab (Mathworks) or ImageJ (National Institutes of Health).

To quantify the spread of sensory-evoked signal over the cortex, both cortical hemispheres were divided into 10 distinct regions (square regions of 0.11 mm^2), including (*i*) anterior cingulate (dorsal part) and anterior segment of secondary motor cortex ($M2_A$), (*ii*) forelimb primary somatosensory cortex (FL), (*iii*) anterior cingulate (dorsal and ventral part) and posterior segment of secondary motor cortex (M2p), (*iv*) hindlimb somatosensory cortex (HL), (*v*) C2 primary barrel cortex, (*vi*) parietal association cortex (ptA), (*vii*) retrosplenial cortex (RS), (*viii*) primary visual cortex (V1), (*ix*) secondary visual cortex (V2), and (*x*) primary motor cortex (M1). All cortical regions were identified based on stereotaxic coordinates (7) and their stereotyped position relative to the functionally defined hindlimb (HL) area. In all experiments, the functional locations of the left and right forelimb maps were confirmed using forelimb-evoked VSD responses.

To assess stroke size, maps of blood flow change were created by measuring the difference in speckle signals in both cortical hemispheres before, and after targeted ischemia to individual pial arterioles that supplied the right primary forelimb sensory representation. Thresholding (50% of the maximal laser speckle contrast value) was used to define the map borders (4, 8). For consistency, we excluded experiments in which the area covered by stroke was larger than 1 mm^2. No changes were observed in the blood flow map in the contralesional hemisphere.

Cortical EEG Recording. A Teflon-coated chlorided silver wire (0.125 mm) was placed on the cortical surface. A reference electrode was placed on the nasal bone. The cortical signal was amplified and filtered (0–1,000 Hz) using a DC amplifier.

Local Field Potential Recording. The local field potential (LFP) was recorded by inserting a glass pipette (5–10 MΩ) into either the center of primary forelimb cortex (at 250–500 μm depth) or within one of three thalamic nuclei (the ventral posterolateral, the ventral posteromedial, or the posterior medial nucleus). The signal was amplified by an Axopatch 200A (Axon Instruments) and filtered from DC to 1,000 Hz. The forelimb cortex was identified based on the VSD fluorescence signal. The thalamic nuclei were localized based on stereotaxic coordinates (7) and their stereotyped position relative to the bregma. The recording positions were confirmed by recording the extracellular synaptic potentials evoked by stimulating the contralateral forelimb.

Local Pharmacology. Local silencing was performed by pressure injection (30–60 s, 20–40 psi, Picospritzer II; General Valve) of ~0.12 μL 30 μM tetrodotoxin dissolved in an artificial cerebrospinal fluid (ACSF) solution.

Statistical Analysis. One-way ANOVA analysis, adjusted by Bonferroni corrections, was used to compare the amplitude, time to peak, and integral of the VSD-evoked response. All P values ≤ 0.05 were considered statistically significant ($^*P < 0.05$; $^{**}P < 0.01$; $^{***}P < 0.001$). All of the data are expressed as mean ± SE.

1. Mohajerani MH, McVea DA, Fingas M, Murphy TH (2010) Mirrored bilateral slow-wave cortical activity within local circuits revealed by fast bihemispheric voltage-sensitive dye imaging in anesthetized and awake mice. *J Neurosci* 30:3745–3751.
2. Shoham D, et al. (1999) Imaging cortical dynamics at high spatial and temporal resolution with novel blue voltage-sensitive dyes. *Neuron* 24:791–802.
3. Sigler A, Goroshkov A, Murphy TH (2008) Hardware and methodology for targeting single brain arterioles for photothrombotic stroke on an upright microscope. *J Neurosci Methods* 170:35–44.
4. Sigler A, Mohajerani MH, Murphy TH (2009) Imaging rapid redistribution of sensory-evoked depolarization through existing cortical pathways after targeted stroke in mice. *Proc Natl Acad Sci USA* 106:11759–11764.
5. Zhang S, Murphy TH (2007) Imaging the impact of cortical microcirculation on synaptic structure and sensory-evoked hemodynamic responses in vivo. *PLoS Biol* 5:e119.
6. Briers JD, Webster S (1996) Laser Speckle Contrast Analysis (LASCA): A nonscanning, full-field technique for monitoring capillary blood flow. *J Biomed Opt* 1:174–179.
7. Paxinos G, Franklin KBJ (2004) *The Mouse Brain in Stereotaxic Coordinates* (Elsevier, Amsterdam).
8. Baron JC (2001) Perfusion thresholds in human cerebral ischemia: Historical perspective and therapeutic implications. *Cerebrovasc Dis* 11(Suppl 1):2–8.

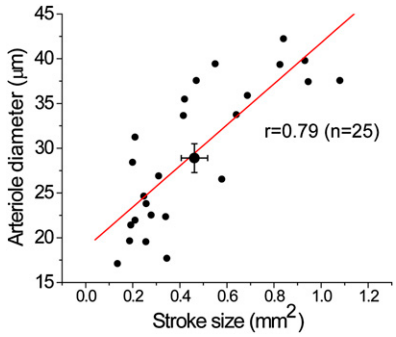

Fig. S1. Relationship between stroke size and diameter of the arteriole blocked to produce ischemic stroke. Focal ischemic strokes are produced by photothrombotic blockage of a single pial arteriole in the forelimb area of the mouse somatosensory cortex. To assess stroke size, maps of blood flow change were made by measuring the difference in laser speckle signals before and after ischemia (*Methods*). Plot shows a linear relationship between the size of strokes and arterioles diameter targeted in our experiments.

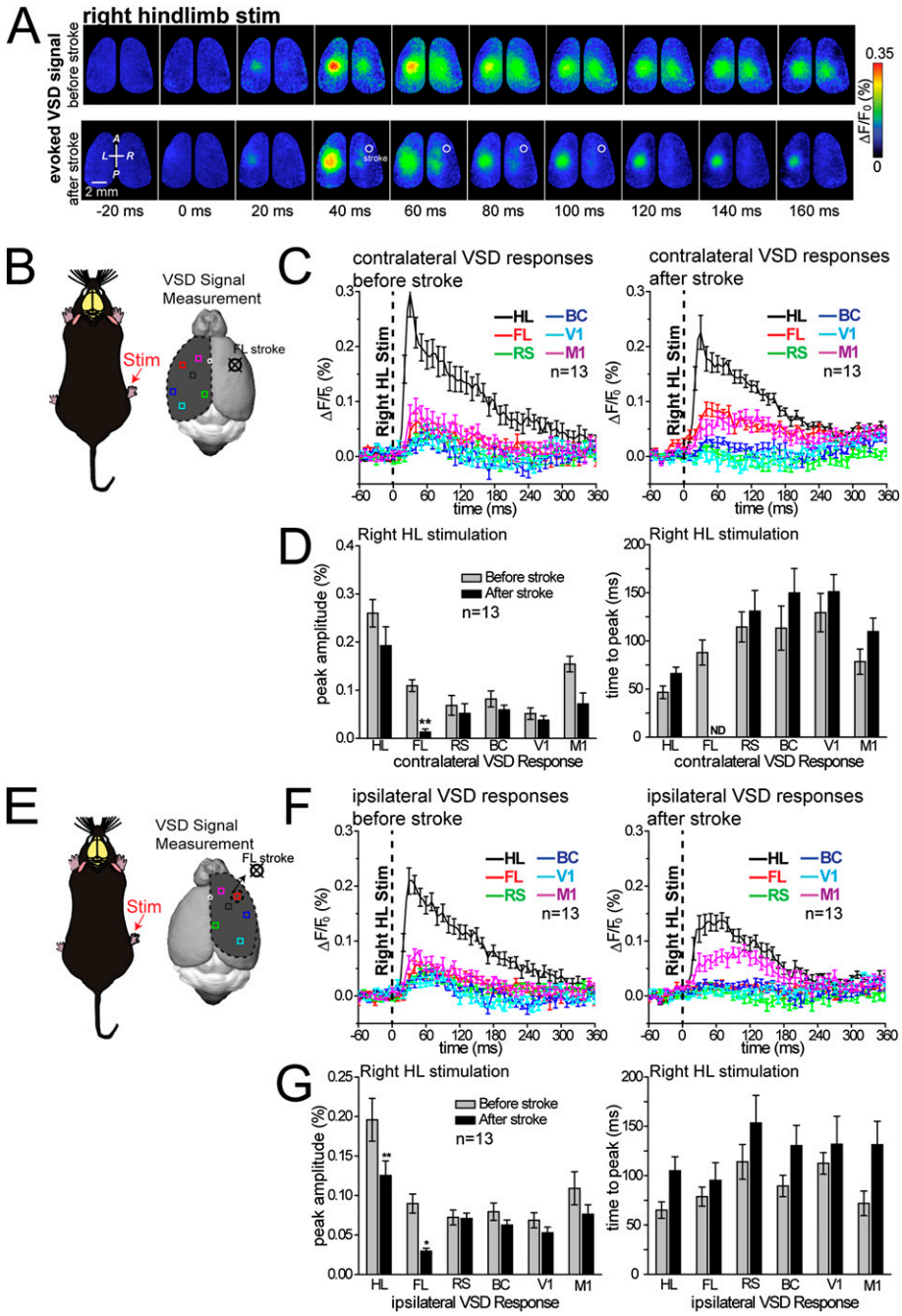

Fig. S2. Stroke in forelimb region did not lead to interhemispheric rearrangements of hindlimb sensory-evoked activity. (*A*) Montage of VSD fluorescence signal in response to tactile stimulation of the right hindlimb in control (*Upper*) and 40 min (*Lower*) after creation of photothrombotic stroke within the right forelimb map outlined with white circles. (*B*) Schematic showing the location of regions of interest within the unaffected hemisphere used for assessing responses to the right hindlimb. (*C*) Plots of average VSD response measured within the nonaffected hemisphere (stroke in other hemisphere). (*D*) Quantification of the VSD signal response peak amplitude and time to peak in *C*. Note that right HL stimulation-evoked contralateral signals were unchanged within the stroke-unaffected hemisphere. (*E*) Cartoon showing the regions of interest within affected hemispheres that were used for assessing responses to the right hindlimb. (*F* and *G*) Same as *C* and *D* except that the VSD signals were measured within the stroke-affected hemisphere (n = 13 mice; $^{*}P < 0.05$; $^{**}P < 0.01$; $^{***}P < 0.005$).

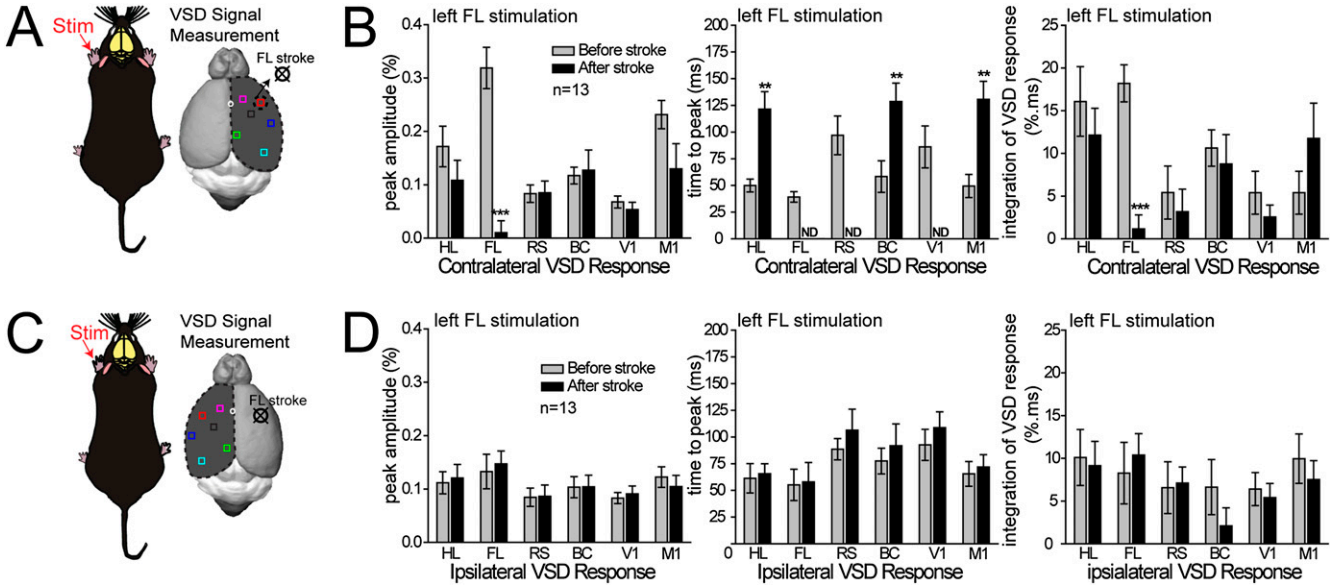

Fig. S3. Quantification of kinetics and amplitude of VSD response to stimulation of left forelimb before and after acute stroke. Based on data also shown in Fig. 2, we measured amplitude, time to peak, and amplitude integral of contralateral and ipsilateral VSD responses to tactile forelimb stimulation. (*A* and *C*) Schematics showing the locations of regions of interest (hindlimb, forelimb, retrosplenial, barrel, and visual and motor cortex) within the (*A*) right (contralateral to stimulated limb) and (*C*) left (ipsilateral to stimulated limb) hemispheres used for assessing responses to the left forelimb. (*B* and *D*) Statistical quantification of contralateral (*B*) and ipsilateral (*D*) VSD response change to stimulation of left forepaw before and after forelimb cortex stroke within the right hemisphere. Peak amplitudes, time to peak, and integral of the VSD response signal amplitude (area under the curve; t = 0–200 ms). VSD signal intensities were averaged for regions of interest with an area of 0.11 mm^2 (n = 13 mice; $^*P < 0.05$; $^{**}P < 0.01$; $^{***}P < 0.005$).

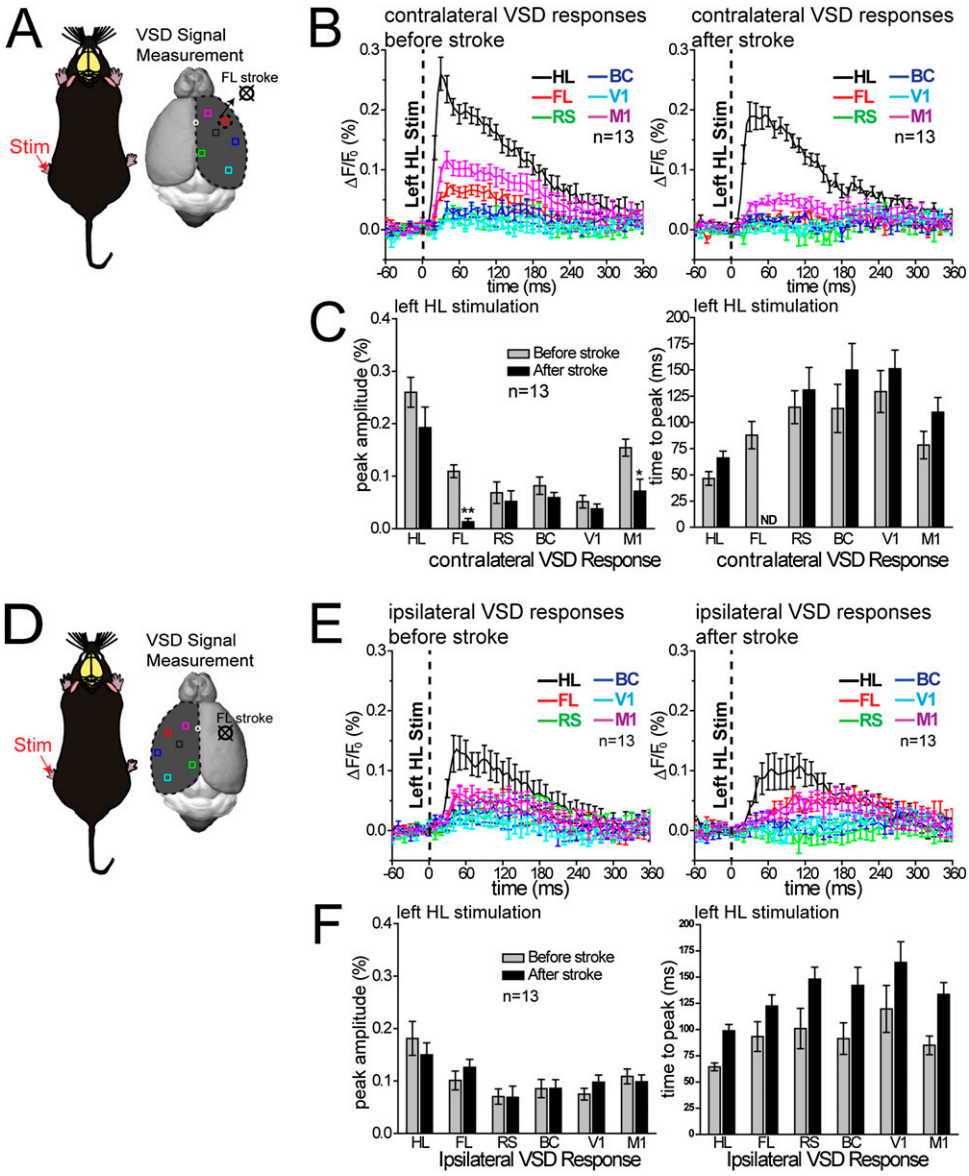

Fig. S4. Stroke in forelimb region did not change the hindlimb sensation-evoked response. Targeted ischemia was created within forelimb area as in Fig. 1, and VSD responses were monitored in both cortical hemispheres in response to stimulation of the left hindlimb. (*A*) Schematic showing the location of regions of interest within the right hemisphere used for assessing responses to the left hindlimb. (*B*) Plots of average VSD response measured within the stroke-affected hemisphere in response to stimulation of the left hindlimb before and after stroke made within right forelimb. (*C*) Quantification of the VSD signal response peak amplitude and time to peak before and after creation of acute stroke. Notice that HL stimulation-derived contralateral signals were unchanged within stroke-affected hemisphere except for motor cortex and the ischemic forelimb area. (*D*) Cartoon showing the regions of interest within the unaffected hemisphere that were used for assessing responses to the left hindlimb. (*E* and *F*) Same as *B* and *C* except that the VSD signals were measured within stroke-unaffected hemispheres (n = 13 mice; $^{*}P < 0.05$; $^{**}P < 0.01$; $^{***}P < 0.005$).

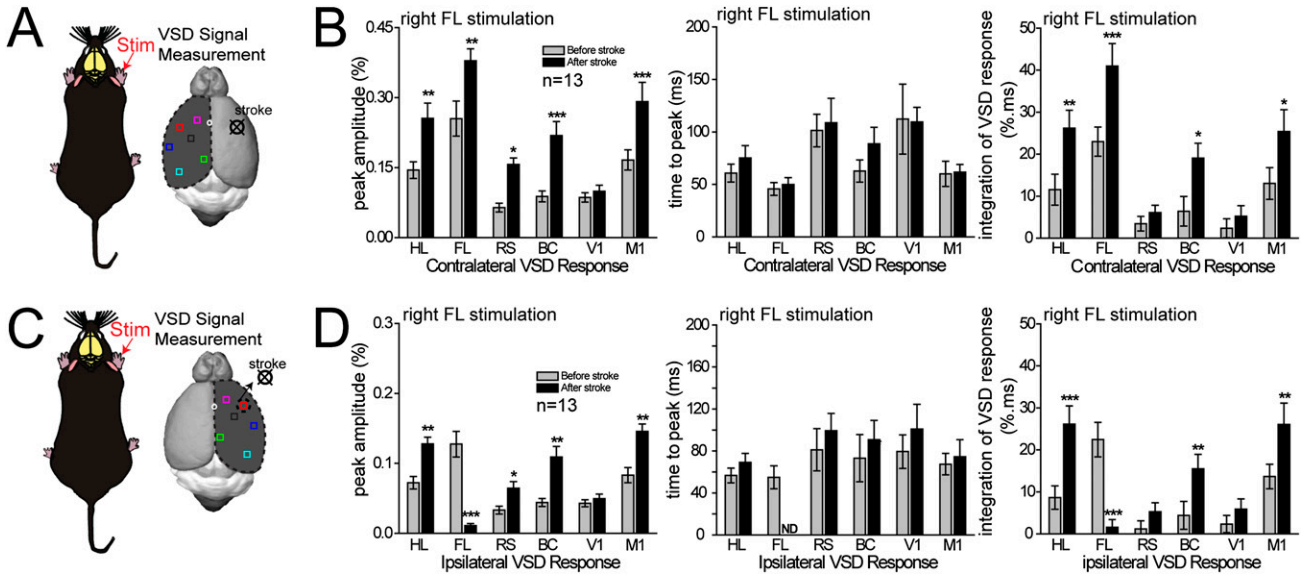

Fig. S5. Quantification of kinetics and amplitude of the VSD response to stimulation of the unaffected (right) forelimb before and after acute stroke. Based on data also shown in Fig. 3, we measured amplitude, time to peak, and amplitude integral of contralateral and ipsilateral VSD fluorescence responses to tactile stimulation of the unaffected forelimb. (*A* and *C*) Graphic showing the location of six regions of interest within the (*A*) left (unaffected) hemisphere (contralateral to stimulated limb) and (*C*) right (affected) hemisphere (ipsilateral to stimulated limb) used for assessing responses to the unaffected forelimb. (*B* and *D*) Quantification of contralateral (*B*) and ipsilateral (*D*) VSD response change to stimulation of unaffected forepaw before and after creation of forelimb cortex stroke within the right hemisphere. Peak amplitudes, time to peak, and integral of the VSD response signal amplitude. VSD signal intensities were averaged for regions of interest with an area of 0.11 mm^2 (n = 13 mice; $*P < 0.05$; $**P < 0.01$; $***P < 0.005$).

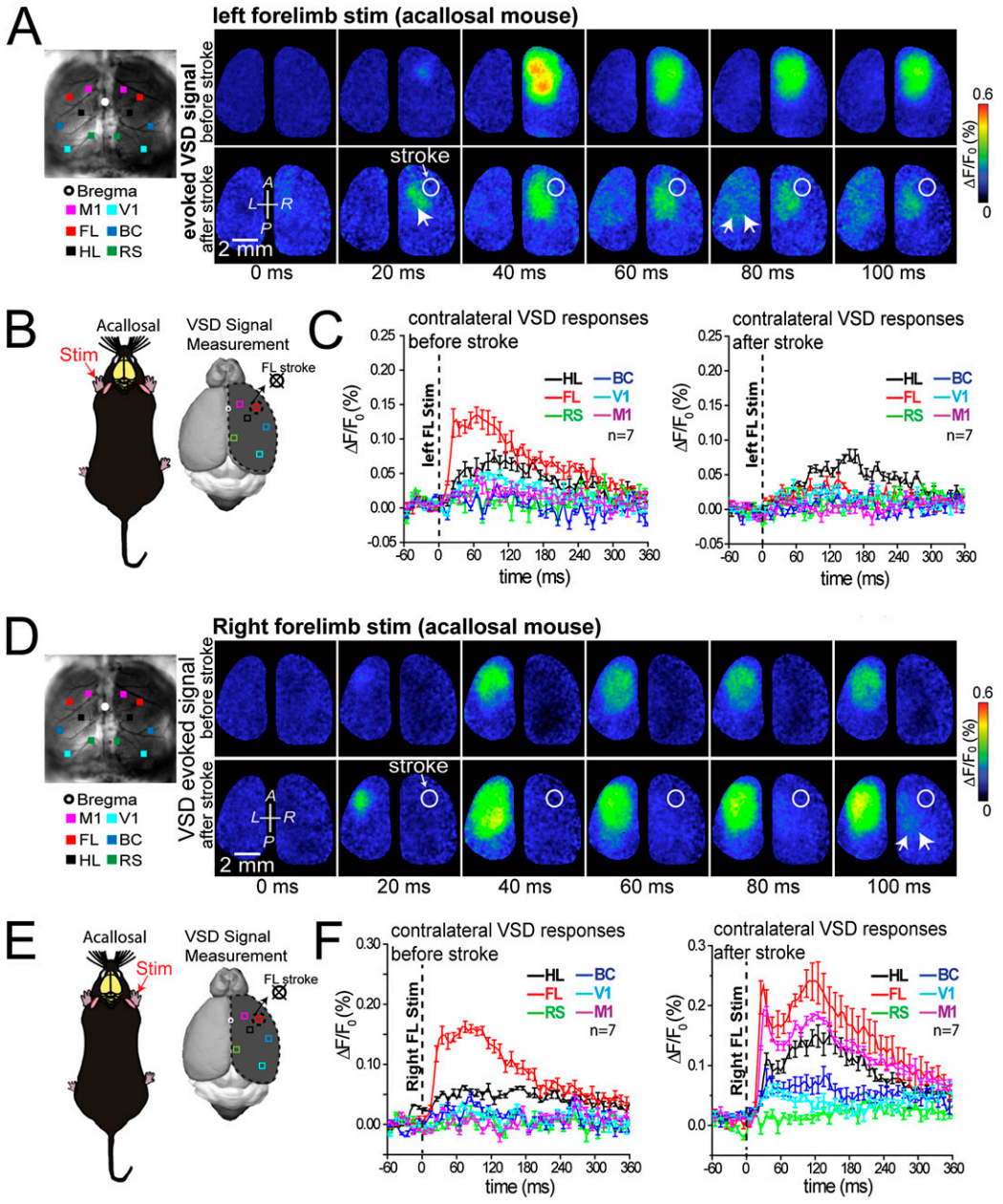

Fig. S6. Bilateral changes in sensory processing in response to stroke are apparent in I/LnJ acallossal mice. (*A Left*) Targeted ischemia was made as in Fig. 1. (*A Upper Right*) Images of left forelimb-stimulated sensory responses before and 40 min after targeted ischemia (*Lower Right*) (stroke focus outlined in white) to the right hemisphere forelimb map. (*B* and *C*) Regions of interest and quantitative data ($n = 7$) for stimulation of the stroke-affected paw and measurement of responses within the stroke-affected hemisphere. (*D*) Images of sensory response mediated by stimulation as in *A* but from the unaffected forelimb of an acallossal mouse before and after ischemic stroke. (*E* and *F*) Regions of interest and quantification of responses within the unaffected hemisphere mediated by the unaffected forelimb (right) 40 min after targeted stroke in acallossal mice ($n = 7$). Contralateral VSD signals measured over several cortical regions in responses to left forelimb stimulation changed significantly after focal stroke.

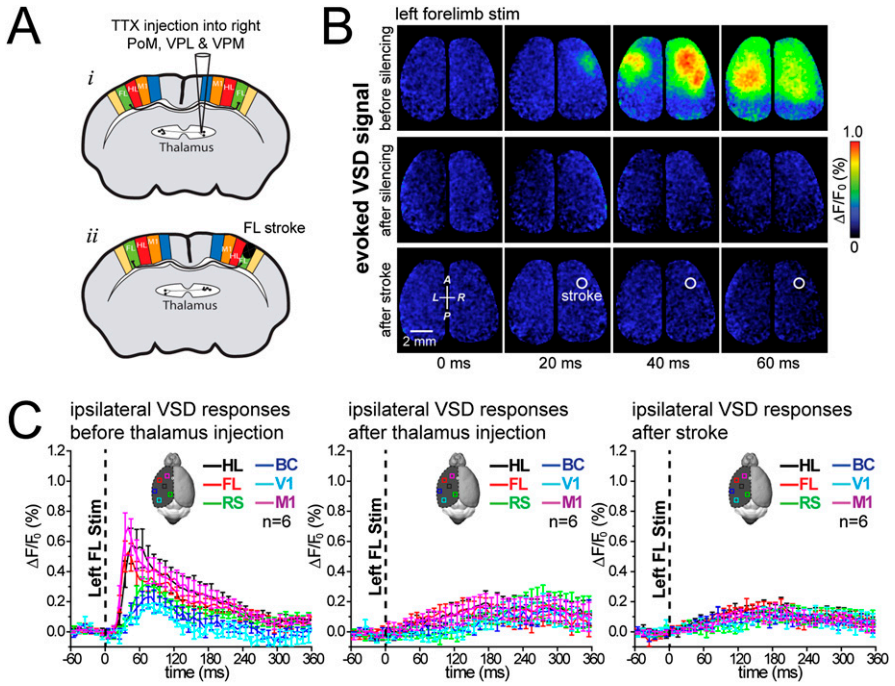

Fig. S7. Routing of ipsilateral sensory signals from the stroke-affected paw to the unaffected hemisphere is dependent on interhemispheric thalamic connections. (*A*) As shown in Fig. 6, right thalamic nuclei were first inactivated to inhibit interhemispheric thalamic connections before creation of ischemic stroke within the forelimb sensory map. (*B*) Montages of VSD images before stroke (*Top*), after tetrodotoxin (30 μM) injection into the thalamus (*Middle*), and after creation of ischemia within the right forelimb area (*Bottom*). (*C*) Quantification of left forelimb ipsilaterally evoked responses as explained in *B*. As expected, silencing the contralateral thalamus blocked both the contralateral and ipsilateral cortical signal. Note that creation of stroke after the thalamus is inactivated does not preserve ipsilateral responses.

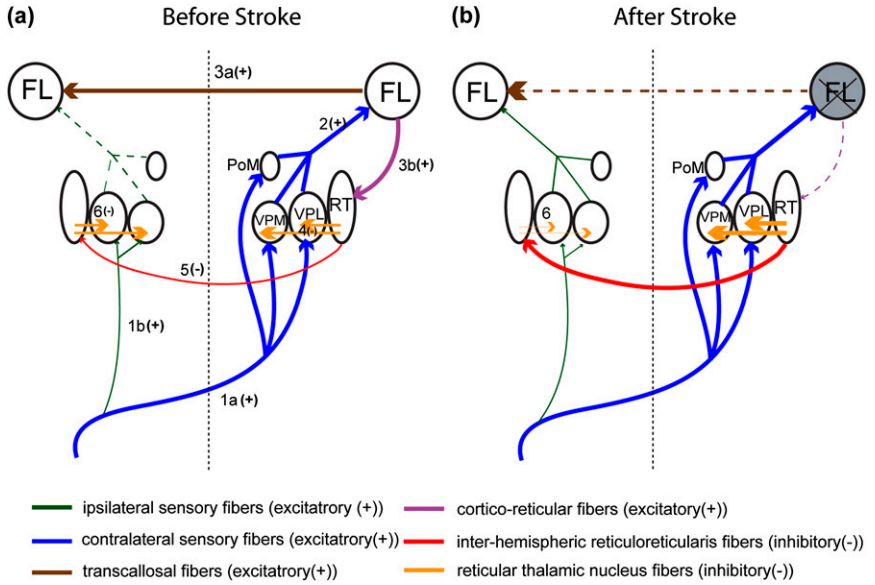

Fig. S8. Cartoon showing detailed diagram of possible interhemispheric rerouting of sensory processing within the first hours of targeted ischemia to the forelimb sensory map. (*A*) Before stroke, excitatory connections travel contralaterally (1a) and ipsilaterally (1b) from the limb to the thalamic nuclei [ventral posteriolateral (VPL), ventral posteriomedial (VPM), and posterior medial nucleus (PoM)]. VPL, VPM, and PoM nuclei of the thalamus make excitatory projections to the somatosensory cortex (2), and from the cortex, excitatory connections travel through the corpus callosum to the homotopic contralateral cortex (3a). There is also excitatory input from the cortex to the reticular nucleus (RT) of the thalamus in the same hemisphere (3b) (1) along with cortical feedback to the VPL and VPM nuclei. RT inhibits the VPL and VPM nuclei of the thalamus (4). RT nuclei are also connected through commissural fibers and exert inhibitory influences on each other (5) (2–7). (*B*) Cortical damage after ischemic stroke produces an increase of the firing frequency of ipsilesional thalamic reticular neurons (8), which translates to enhanced inhibition of VPL and VPM nuclei within the same hemisphere (4) and RT neurons within opposite hemisphere (contralesional; 5). This enhanced inhibition of contralesional RT neurons may lead to disinhibition of contralesional VPL, VPM, and PoM nuclei (6) and thus, unmask the ipsilateral sensory pathway (1b). Decreased inhibition from the contralesional RT nucleus (6) after stroke may contribute to the redistribution of sensory processing within the first hour after stroke (Fig. 7).

1. Golshani P, Liu XB, Jones EG (2001) Differences in quantal amplitude reflect GluR4- subunit number at corticothalamic synapses on two populations of thalamic neurons. *Proc Natl Acad Sci USA* 98:4172–4177.
2. Chen S, Raos V, Bentivoglio M (1992) Connections of the thalamic reticular nucleus with the contralateral thalamus in the rat. *Neurosci Lett* 147:85–88.
3. Raos V, Bentivoglio M (1993) Crosstalk between the two sides of the thalamus through the reticular nucleus: A retrograde and anterograde tracing study in the rat. *J Comp Neurol* 332: 145–154.
4. Battaglia G, Lizier C, Colacitti C, Princivalle A, Spreafico R (1994) A reticuloreticular commissural pathway in the rat thalamus. *J Comp Neurol* 347:127–138.
5. Rinvik E (1984) Thalamic commissural connections in the cat. *Neurosci Lett* 44:311–316.
6. Paré D, Steriade M (1993) The reticular thalamic nucleus projects to the contralateral dorsal thalamus in macaque monkey. *Neurosci Lett* 154:96–100.
7. Timofeev I, Steriade M (1996) Low-frequency rhythms in the thalamus of intact-cortex and decorticated cats. *J Neurophysiol* 76:4152–4168.
8. Bures J, Buresova O, Weiss T, Fifkova E (1963) Excitability changes in non-specific thalamic nuclei during cortical spreading depression in the rat. *Electroencephalogr Clin Neurophysiol* 15:73–83.

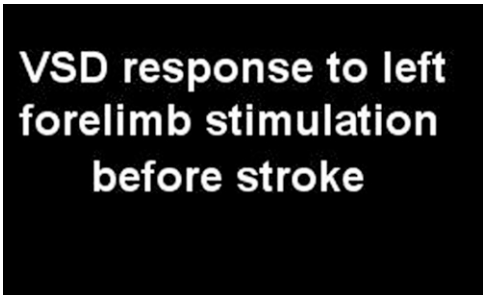

Movie S1. Sensation-evoked response imaged across of both cortical hemispheres with voltage-sensitive dye in a urethane-anesthetized C57BL6J mouse before and after creation of photothrombotic ischemia within the right forelimb map. For reference purposes, we outlined the ischemic region using a white circle. Images were captured with a time resolution of 5 ms. VSD responses were imaged before and after stimulation of the left forelimb with a single 5-ms tap. Data presented were generated from the average of 20 trials of stimulation and are presented as $\Delta F/F_0$ (%).

Movie S1

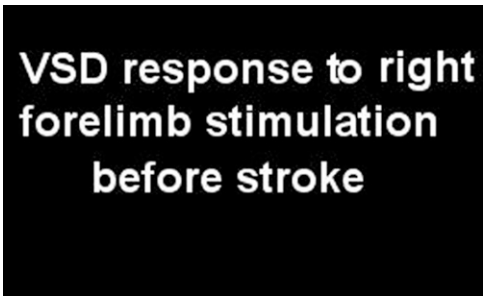

Movie S2. Similar to Movie S1 except that the VSD signals (before and after stroke) were imaged in response to stimulation of right forelimb.

Movie S2